scientific reports

Check for updates

OPEN

Vibration control of a nonlinear cantilever beam operating in the 3D space

Phuong-Tung Pham[1,2], Quoc Chi Nguyen[1], Mahnjung Yoon[3] & Keum-Shik Hong[2]✉

This paper addresses a control problem of a nonlinear cantilever beam with translating base in the three-dimensional space, wherein the coupled nonlinear dynamics of the transverse, lateral, and longitudinal vibrations of the beam and the base's motions are considered. The control scheme employs two control inputs applied to the beam's base to control the base's position while simultaneously suppressing the beam's transverse, lateral, and longitudinal vibrations. According to the Hamilton principle, a hybrid model describing the nonlinear coupling dynamics of the beam and the base is established: This model consists of three partial differential equations representing the beam's dynamics and two ordinary differential equations representing the base's dynamics. Subsequently, the control laws are designed to move the base to the desired position and attenuate the beam's vibrations in all three directions. The asymptotic stability of the closed-loop system is proven via the Lyapunov method. Finally, the effectiveness of the designed control scheme is illustrated via the simulation results.

The systems consisting of an elastic cantilever beam fixed on a translating base are found in various practical engineering applications, such as master fuel assemblies in nuclear refueling machines, robotic manipulators[1], and micro-electro-mechanical systems[2–4]. In these systems, the base's translational motion can produce large-amplitude vibrations of the beam in the three-dimensional (3D) space. This vibration becomes a significant negative factor in association with the system's safety and performance. Therefore, it is necessary to analyze and control the 3D vibration of the beam, operated by a moving base, to ensure safety and performance.

The flexible cantilever beam is a distributed parameter system with an infinite number of vibration modes. Its dynamics are characterized by partial differential equations (PDEs)[5–8]. When a flexible beam is fixed on a translating base, the base's dynamics (as a lumped parameter system) are described by ordinary differential equations (ODEs) to be considered simultaneously with the beam's dynamics. Furthermore, if the amplitudes of the beam's vibrations are large, 3D analysis of the beam's dynamics should be performed; wherein the nonlinear coupling effects between the transverse, lateral, and longitudinal vibrations are considered, see Fig. 1.

The dynamic behaviors of the beam attached to a moving base have been studied in the literature[9–12]. Park et al. developed an equation of motion of the mass-beam-cart system, which is a beam with translating base, based on the Hamilton principle[13]. The system's natural frequencies were also obtained by using modal analysis. Later, the vibration of a flexible beam fixed on a cart and carrying a moving mass was examined via an experimental study[14]. However, most researches on the beam attached to a translating base assume that the base moves along one direction, restricting the beam's vibration to a two-dimensional space. In these works, only the transverse vibration was considered. For the beam with a translating base in the 3D space, Shah and Hong addressed the vibration problem of the master fuel assembly in nuclear refueling machines[15]. In their work, the nuclear fuel rod and the trolley, respectively, were treated as a flexible beam and a carrying base moving on the horizontal plane.

The control problem of distributed parameter systems, whose dynamics is described by PDEs, has been investigated in the literature[16–21]. Boundary control technique, wherein the control input is exerted to the PDE through its boundary conditions[22–25], is a powerful tool for handling these systems. Contrary to the stationary beam, the vibration of the cantilever beam with a moving base can be suppressed via the control input applied at the base (i.e., the clamped end of the beam) or the beam's tip. In this situation, we aim to simultaneously control of the base's position and the beam's vibration. These objectives can be achieved by either open-loop control[26,27] or closed-loop control[15,28–33]: The input shaping control is the most feasible and practical open-loop control technique for beams with a moving base. In a study published by Shah et al.[26], model parameters of an underwater

[1]Department of Mechatronics, Faculty of Mechanical Engineering, Ho Chi Minh City University of Technology (HCMUT), VNU-HCM, Ho Chi Minh City, Vietnam. [2]School of Mechanical Engineering, Pusan National University, Busan 46241, South Korea. [3]POWER MnC Co., Ltd., Ulsan 44988, South Korea. ✉email: kshong@pusan.ac.kr

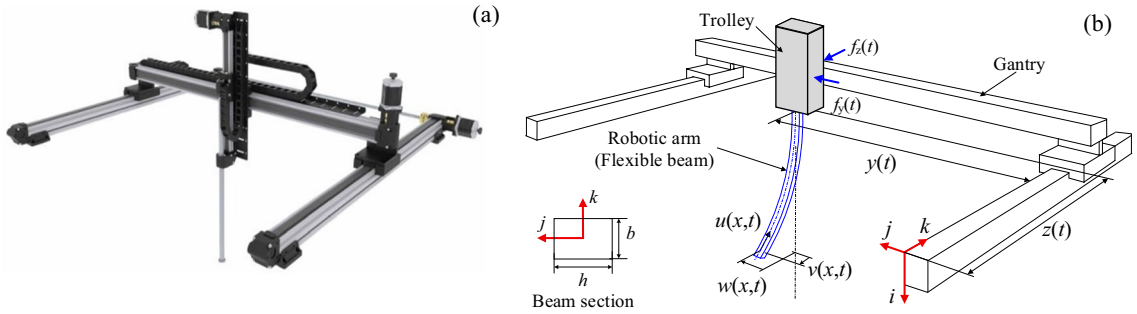

Figure 1. An example of nonlinear cantilever beams operating in the 3D space: (**a**) Gantry robot. (www.a-m-c.com/servo-drives-for-gantry-systems), (**b**) the defined coordinate system and motions.

system consisting of a beam and a translating base were determined using the model analysis method. Accordingly, the input shaping control law was designed to position the base and suppress the beam's vibration. Pham et al.[27] used the model parameters obtained through an experiment to design the input shaping control law for a non-uniform beam with a moving base. For the closed-loop control technique, Liu and Chao presented an experimental study on implementing the neuro-fuzzy approach to control a beam-cart system[28]. In their work, the piezoelectric transducers located at the beam's tip were used to suppress the transverse vibration. Another closed-loop control of an Euler–Bernoulli beam with a translating base was done by Shah and Hong[15], whereas the control of a Timoshenko beam attached to a moving base was presented by Pham et al.[34].

Most studies on controlling the flexible beam attached to a translating base considered only the linear vibrations[15,26–28]. Under the assumption of small-amplitude vibration, the dynamic tension was ignored. However, in the case of large-amplitude vibrations, the negligence of the dynamic tension (which makes the beam's dynamics nonlinear) can affect the system's performance and stability. Also, the existing studies assumed that the beam's vibration occurred in a plane. Thus, only the transverse or lateral vibrations were considered. Even though Shah and Hong[15] investigate both the transverse and lateral vibrations of an Euler–Bernoulli beam, they ignored the coupled dynamics of the transverse and lateral vibrations; that is, the transverse vibration does not affect the time-evolution of the lateral vibration and vice versa.

Recently, the 3D vibration analysis of a beam has received significant attention[35–40]. Do and Pan[38] and Do[39] used the Euler–Bernoulli beam model with large-amplitude vibrations to model a flexible riser. The authors obtained a model describing the system's transverse, lateral, and longitudinal vibrations. He et al.[41], Ji and Liu[42,43], and Liu et al.[44] investigated the coupled dynamics of a 3D cantilever beam with a tip payload described by a set of PDEs and ODEs. Also, control problems of 3D beams, wherein the coupled dynamics of nonlinear vibrations, were investigated in the literature. However, these studies have either dealt with a beam attached to a stationary base or proposed control strategies wherein control forces/torques were applied to the beam's tip. The implementation of control actions at the tip is not feasible or practical, see Fig. 1. It might be possible to put an actuator at the tip of a large cantilever beam of a space structure or a riser system. But, for gantry manipulators, surgeon robots, and flexible liquid handling robots, implementing the control forces/torques in the tip is not possible because the tip has to interact with an object or the environment.

The published papers in the literature on controlling cantilever-beam vibrations are restricted to: (i) The cases where the cantilever is affixed on a stationary base, and the free end has 3D motions[41–44]; and (ii) the beam is attached to a translating base, but the considered dynamics are linear by ignoring the coupled dynamics between the transversal and lateral vibrations of the beam[15,26–28]. Thus, the control problem of a nonlinear cantilever beam operating in the 3D space without using control input at the tip has not been solved yet.

In this paper, the beam's longitudinal vibration and axial deformation (which makes the beam's dynamics nonlinear) are further considered. In such cases of large-amplitude vibrations, the omission of longitudinal vibration and axial deformation can affect the system's performance and lead to an erroneous result. Henthforth, the control problem of the nonlinear 3D vibrations of a beam affixed on a translating base without any additional actuators is addressed for the first time. The considered system is represented as a gantry robot consisting of the gantry, trolley, and flexible robotic arm depicted in Fig. 1. In the gantry robot, the gantry moves along the k-axis, whereas the trolley moves along the j-axis. A flexible robotic arm with a constant length is fixed to the trolley. The Hamilton principle is used to develop a novel hybrid model describing the nonlinear coupling dynamics of the robotic arm's transverse, lateral, and longitudinal vibrations, and the rigid body motions of the gantry and trolley. Employing the Lyapunov method, boundary control laws are developed for simultaneous control of the trolley's position, the gantry's position, and the robotic arm's 3D vibrations. The asymptotic stability of the closed-loop system is verified. Finally, the simulation results are provided.

The main contributions of this paper are summarized as follows: (i) A novel dynamic model of a flexible beam attached to a translating base, wherein the coupled dynamics of the nonlinear transverse, lateral, and longitudinal vibrations and the base's motions are developed for the first time. (ii) A boundary control strategy using the control forces at the base for simultaneous position control and vibration suppression is designed. (iii) The asymptotic stability of the closed-loop system is proven by using the Lyapunov method, and simulation results are provided.

Problem formulation

In Fig. 1, a flexible robotic arm is modeled as a uniform Euler–Bernoulli beam of length l. The motions of the gantry and trolley are generated by two control forces f_z and f_y, respectively. The positions of the trolley and gantry are denoted by $y(t)$ and $z(t)$, respectively. The beam's vibrations in the i, j, and k axes are defined as the longitudinal vibration $u(x, t)$, the transverse vibration $w(x, t)$, and the lateral vibration $v(x, t)$, respectively. In this study, the subscripts x and t, i.e., $(\cdot)_x$ and $(\cdot)_t$, are the partial derivatives with respect to x and t, respectively, whereas $\dot{y}$ and $\dot{z}$ denotes the total derivative of $y(t)$ and $z(t)$ in t, respectively. The kinetic energy of the entire gantry, trolley, and beam system is given as follows:

$$K = \frac{1}{2}\rho A \int_0^l \left[\left(y + w_t\right)^2 + u_t^2 + \left(z + v_t\right)^2 \right] dx + \frac{1}{2}(m_1 + m_2)\dot{y}^2 + \frac{1}{2}m_2\dot{z}^2 \tag{1}$$

where ρ and A are the beam's mass density and cross-sectional area; m_1 and m_2 are the gantry's mass and trolley's mass, respectively. The potential energy due to the axial force, the axial deformation, and the bending moment is given as follows:

$$U = \int_0^l P(x)\left(\frac{w_x^2}{2} + \frac{v_x^2}{2}\right) dx + \frac{1}{2}\int_0^l EA\varepsilon(x,t)^2 dx + \frac{1}{2}EI_y \int_0^l w_{xx}^2 dx + \frac{1}{2}EI_z \int_0^l v_{xx}^2 dx \tag{2}$$

where $P(x) = \rho A(l - x)g$ is the axial force generated by the influence of the gravitational acceleration on the beam's elements[45,46], E denotes Young's modulus, and I_y and I_z indicate the moments of inertia of the beam. The axial strain $\varepsilon(x, t)$ is given by the following approximation[47]:

$$\varepsilon(x,t) = u_x + w_x^2/2 + v_x^2/2. \tag{3}$$

The virtual work done on the system by the boundary control inputs and the friction is given as follows.

$$\delta W = f_y \delta y + f_z \delta z - c_w \int_0^l w_t \delta w dx - c_u \int_0^l u_t \delta u dx - c_v \int_0^l v_t \delta v dx \tag{4}$$

where c_w, c_u, and c_v are the structral damping coefficients (i.e., the subscripts w, u, and v stand for transverse, longitudinal, and lateral, respectively). According to Hamilton's principle, the dynamic model of the considered system and the corresponding boundary conditions are obtained as follows.

$$\rho A(\ddot{y} + w_{tt}) + c_w w_t - (Pw_x)_x - EA[w_x(u_x + w_x^2/2 + v_x^2/2)]_x + EI_y w_{xxxx} = 0, \tag{5}$$

$$w(0,t) = w_x(0,t) = w_{xx}(l,t) = w_{xxx}(l,t) = 0, \tag{6}$$

$$\rho A u_{tt} + c_u u_t - EA[u_x + w_x^2/2 + v_x^2/2]_x = 0, \tag{7}$$

$$u(0,t) = u_x(l,t) + w_x^2(l,t)/2 + v_x^2(l,t)/2 = 0, \tag{8}$$

$$\rho A(\ddot{z} + v_{tt}) + c_v v_t - (Pv_x)_x - EA[v_x(u_x + w_x^2/2 + v_x^2/2)]_x + EI_z v_{xxxx} = 0, \tag{9}$$

$$v(0,t) = v_x(0,t) = v_{xx}(l,t) = v_{xxx}(l,t) = 0, \tag{10}$$

$$(m_1 + m_2)\ddot{y} - c_w \int_0^l w_t dx + EI_y w_{xxx}(0,t) = f_y, \tag{11}$$

$$m_2\ddot{z} - c_v \int_0^l v_t dx + EI_z v_{xxx}(0,t) = f_z. \tag{12}$$

The dynamics of the considered system are represented by the nonlinear PDE-ODE model in (5)–(12): Eqs. (5)–(10) are PDEs describing the transverse, longitudinal, and lateral vibrations of the robotic arm, respectively, whereas the ODEs in (11) and (12) represent the dynamics of the gantry and the trolley, respectively. Observably, the beam's motion affects the gantry and trolley's motions and vice versa. Additionally, if the potential energy caused by the axial deformation is ignored (i.e., $\varepsilon^2 = (u_x + w_x^2/2 + v_x^2/2)^2 \cong 0$), the nonlinear terms in (5), (7), and (9) vanish. Then, the coupling dynamics between the transverse, lateral, and longitudinal vibrations can be decoupled.

Controller design

The two control objectives are position control and vibration suppression: (i) Move the gantry and trolley carrying the flexible beam to the desired positions, and (ii) suppress the beam's transverse, lateral, and longitudinal vibrations. In this paper, two forces f_z and f_y applied to the gantry and trolley are used as the control inputs to achieve the control objectives. The position errors of the trolley and gantry are defined as follows:

$$e_y = y - y_{\mathrm{d}}, \tag{13}$$

$$e_z = z - z_{\mathrm{d}} \tag{14}$$

where y_{d} and z_{d} are the desired positions of the trolley and gantry, respectively. Based on the Lyapunov direct method, we design f_z and f_y to guarantee that the convergences of the vibrations, position errors, and velocities of the trolley and gantry to zero are achieved. The following control forces are proposed to stabilize the considered system.

$$f_y = -K_1\dot{y} - K_2 e_y - K_3 w_{xxx}(0,t), \tag{15}$$

$$f_z = -K_4\dot{z} - K_5 e_z - K_6 v_{xxx}(0,t) \tag{16}$$

where K_i (i=1,2,…,6) are the control parameters. The implementation of these control laws requires the measurement of $w_{xxx}(0, t)$ and $v_{xxx}(0, t)$. In practice, these signals can be obtained by using strain gauge sensors attached at the clamped end of the beam.

The following lemmas and assumptions are used for stability analysis of the closed-loop system with the control laws given in (15) and (16).

Lemma 1 [48]. *Let $\varphi(x,t) \in \mathbb{R}$ be a function defined on $x \in [0,l]$ and $t \in [0,\infty)$ that satisfies the boundary condition $\varphi(0,t) = 0$, $\forall t \in [0,\infty)$, the following inequalities hold.*

$$\int_0^l \varphi^2(x,t)dx \le l^2 \int_0^l \varphi_x^2(x,t)dx,\ \forall x \in [0,l], \tag{17}$$

$$\varphi^2(x,t) \le l \int_0^l \varphi_x^2(x,t)dx,\ \forall x \in [0,l]. \tag{18}$$

Furthermore, if $\varphi(x,t)$ satisfies $\varphi(0,t) = \varphi_x(0,t) = 0$, $\forall t \in [0,\infty)$, then the following inequalities hold.

$$\int_0^l \varphi_x^2(x,t)dx \le l^2 \int_0^l \varphi_{xx}^2(x,t)dx,\ \forall x \in [0,l], \tag{19}$$

$$\varphi^2(x,t) \le l^3 \int_0^l \varphi_{xx}^2(x,t)dx,\ \forall x \in [0,l]. \tag{20}$$

Lemma 2 [49]. *Let $\varphi_1(x,t), \varphi_2(x,t) \in \mathbb{R}$ be a function defined on $x \in [0,l]$. Then, the following inequality holds.*

$$\varphi_1(x,t)\varphi_2(x,t) \le \varphi_1^2(x,t)/\delta + \delta\varphi_2^2(x,t),\ \forall \delta > 0. \tag{21}$$

Lemma 3 [50]. *If $\varphi(x,t)$: $[0,\ l] \times \mathbb{R}^+ \to \mathbb{R}$ is uniformly bounded, $\{\varphi(x,t)\}_{x\in[0,l]}$ is equicontinuous on t, and $\lim_{t\to\infty} \int_0^t \|\varphi(x,\tau)\|^2 d\tau$ exists and is finite, then $\lim_{t\to\infty} \|\varphi(x,t)\| = 0$.*

Assumption 1 [21]. *The transverse vibration $w(x,t)$, the lateral vibration $v(x,t)$, and the longitudinal vibration $u(x,t)$ of a flexible beam satisfy the following inequalities: $u_x^2 \le w_x^2/2$ and $u_x^2 \le v_x^2/2$. By using Lemma 1, we obtain.*

$$\int_0^l u^2 dx \le l^2 \int_0^l u_x^2 dx \le \frac{l^2}{4}\int_0^l w_x^2 dx + \frac{l^2}{4}\int_0^l v_x^2 dx \le \frac{l^4}{4}\int_0^l w_{xx}^2 dx + \frac{l^4}{4}\int_0^l v_{xx}^2 dx. \tag{22}$$

Assumption 2 [51]. *If the potential energy of the system in (2) is bounded for $\forall t \in [0,\infty)$, then $w_{xx}(x,t)$, $w_{xxx}(x,t)$, $v_{xx}(x,t)$, and $v_{xxx}(x,t)$ are bounded for $\forall t \in [0,\infty)$.*

Based on the system's mechanical energy, the following Lyapunov function candidate is introduced:

$$V = V_0 + V_1 \tag{23}$$

where

$$\begin{aligned} V_0 = {} & \frac{\rho A}{2}\left[\int_0^l (\dot{y}+w_t)^2 dx + \int_0^l (\dot{z}+v_t)^2 dx + \int_0^l u_t^2 dx\right] + \left(1+\frac{2\alpha_2}{\rho A}\right)\left[\int_0^l P\left(\frac{w_x^2}{2}+\frac{v_x^2}{2}\right)dx\right. \\ & \left. + \frac{1}{2}EA\int_0^l \left(u_x + \frac{w_x^2}{2} + \frac{v_x^2}{2}\right)^2 dx + EI_y\int_0^l w_{xx}^2 dx + EI_z\int_0^l v_{xx}^2 dx\right] + \frac{1}{2}(m_1+m_2)\dot{y}^2 \\ & + \frac{1}{2}m_2\dot{z}^2 + \frac{1}{2}\alpha_1 e_y^2 + \alpha_2\int_0^l (w_t^2 + u_t^2 + v_t^2)dx + \frac{1}{2}\alpha_3 e_z^2, \end{aligned} \tag{24}$$

$$V_1 = \rho A\beta_1 \int_0^l ww_t dx + \frac{1}{2}\beta_1 c_w \int_0^l w^2 dx + \rho A\beta_2 \int_0^l uu_t dx + \frac{1}{2}\beta_2 c_u \int_0^l u^2 dx + (\beta_3 c_w/\rho A)\int_0^l w\dot{y} dx$$
$$+\beta_3 \int_0^l \dot{y}(\dot{y} + w_t)dx + \beta_4 \dot{y} e_y + \beta_5 \int_0^l e_y(\dot{y} + w_t)dx + \rho A\beta_6 \int_0^l vv_t dx + \frac{1}{2}\beta_6 c_v \int_0^l v^2 dx$$
$$+(\beta_7 c_v/\rho A)\int_0^l v\dot{z} dx + \beta_7 \int_0^l \dot{z}(\dot{z} + v_t)dx + \beta_8 \dot{z} e_z + \beta_9 \int_0^l e_z(\dot{z} + v_t)dx \tag{25}$$

where α_i ($i = 1, 2, 3$) and β_j ($j = 1, 2, \ldots, 9$) are positive coefficients.

Lemma 4 *The Lyapunov function candidate in* (23) *is upper and lower bounded as follows.*

$$0 \le \lambda_1 W_1 \le V \le \lambda_2 W_2 \tag{26}$$

where λ_1 and λ_2 are positive constants, and

$$W_1 = \dot{y}^2 + \dot{z}^2 + \int_0^l w_t^2 dx + \int_0^l u_t^2 dx + \int_0^l v_t^2 dx + \int_0^l w_{xx}^2 dx + \int_0^l v_{xx}^2 dx + e_y^2 + e_z^2, \tag{27}$$

$$W_2 = \dot{y}^2 + \dot{z}^2 + \int_0^l w_t^2 dx + \int_0^l u_t^2 dx + \int_0^l v_t^2 dx + \int_0^l P(w_x^2 + v_x^2)dx + \int_0^l (u_x + w_x^2/2 + v_x^2/2)^2 dx$$
$$+ \int_0^l w_{xx}^2 dx + \int_0^l v_{xx}^2 dx + e_y^2 + e_z^2. \tag{28}$$

Proof of Lemma 4: See Appendix A.

Lemma 5 *Under the control laws* (15) *and* (16), *the time derivative of the Lyapunov function candidate in* (23) *is upper bounded as follows.*

$$\dot{V} \le -\lambda V \tag{29}$$

where λ is a positive constant.

Proof of Lemma 5: See Appendix B.

Theorem 1. *Consider a hybrid system described by* (5)-(12) *under control laws* (15–16) *and Assumptions 1 and 2. Control parameters K_i ($i = 1, 2, \ldots, 6$) are selected to satisfy the conditions in* (A.15)–(A.23), (B.9), (B.17)–(B.22), *and* (B.25)–(B.35). *The asymptotic stability of the closed-loop system in the sense that the transverse vibration $w(x, t)$, lateral vibration $v(x, t)$, longitudinal vibration $u(x, t)$, and position errors* (13) *and* (14) *converge to zero is guaranteed. Additionally, the control laws are bounded.*

Proof of Theorem: Lemma 4 reveals that the Lyapunov function candidate in (23) is a positive definite. According to Lemma 5, we obtain

$$V(t) \le e^{-\lambda t} V(0) \le V(0) < \infty \tag{30}$$

We define the norm of a spatiotemporal function as follows: $\|w(x,t)\| = \left(\int_0^l w^2(x,t)dx\right)^{1/2}$. Using Lemmas 1 and 4 and Assumption 1, the following inequalities are obtained.

$$w^2(x,t) \le l^3 \int_0^l w_{xx}^2(x,t)dx \le l^3 W_1 \le l^3 V/\lambda_1 < \infty, \tag{31}$$

$$v^2(x,t) \le l^3 \int_0^l v_{xx}^2(x,t)dx \le l^3 W_1 \le l^3 V/\lambda_1 < \infty, \tag{32}$$

$$u^2(x,t) \le l \int_0^l u_x^2(x,t)dx \le \frac{1}{2} l \int_0^l w_x^2(x,t)dx \le \frac{1}{2} l^3 \int_0^l w_{xx}^2(x,t)dx \le \frac{1}{2} l^3 V \lambda_1 < \infty, \tag{33}$$

$$e_y^2(t) \le W_1 \le V/\lambda_1 < \infty, \tag{34}$$

$$\dot{e}_y^2(t) \le W_1 \le V/\lambda_1 < \infty, \tag{35}$$

$$e_z^2(t) \le W_1 \le V/\lambda_1 < \infty, \tag{36}$$

$$\dot{e}_z^2(t) \le W_1 \le V/\lambda_1 < \infty. \tag{37}$$

Inequalities (31–37) assure $w(x, t)$, $u(x, t)$, $v(x, t)$, e_y, $\dot{e}_y$, e_z, and $\dot{e}_z$ are all uniformly bounded. Similarly, we also obtain the boundedness of $\|w(x,t)\|^2$, $\|w_t(x,t)\|^2$, $\|u(x,t)\|^2$, $\|u_t(x,t)\|^2$, $\|v(x,t)\|^2$, and $\|v_t(x,t)\|^2$ based on Lemmas 4 and 5.

$$-\|w(x,t)\|^2 \ge -l^4 W_1 \ge -l^4 V/\lambda_1 \ge l^4 \dot{V}/\lambda\lambda_1$$

$$\Rightarrow \lim_{t\to\infty} \int_0^t \|w(x,\tau)\|^2 d\tau \le -l^4 \lim_{t\to\infty} (V(t) - V(0))/\lambda\lambda_1 < \infty, \tag{38}$$

$$-\|v(x,t)\|^2 \ge -l^4 W_1 \ge -l^4 V/\lambda_1 \ge l^4 \dot{V}/\lambda\lambda_1$$

$$\Rightarrow \lim_{t\to\infty} \int_0^t \|v(x,\tau)\|^2 d\tau \le -l^4 \lim_{t\to\infty} (V(t) - V(0))/\lambda\lambda_1 < \infty, \tag{39}$$

$$-\|u(x,t)\|^2 \ge -l^2 \int_0^l u_x^2(x,t)dx \ge -\frac{1}{2} l^2 \int_0^l w_x^2(x,t)dx \ge -\frac{1}{2} l^4 W_1 \ge -\frac{1}{2} l^4 V\lambda_1 \ge \frac{1}{2} l^4 \dot{V}\lambda\lambda_1$$

$$\Rightarrow \lim_{t\to\infty} \int_0^t \|u(x,\tau)\|^2 d\tau \le -\frac{1}{2} l^4 \lim_{t\to\infty} (V(t) - V(0))\lambda\lambda_1 < \infty. \tag{40}$$

Additionally, the following results also imply that $w(x, t)$, $u(x, t)$, and $v(x, t)$ are equicontinuous in t.

$$d\|w(x,t)\|^2/dt = 2\int_0^l w(x,t)w_t(x,t)dx \le \|w(x,t)\|^2 + \|w_t(x,t)\|^2 < \infty, \tag{41}$$

$$d\|v(x,t)\|^2/dt = 2\int_0^l v(x,t)v_t(x,t)dx \le \|v(x,t)\|^2 + \|v_t(x,t)\|^2 < \infty, \tag{42}$$

$$d\|u(x,t)\|^2/dt = 2\int_0^l u(x,t)u_t(x,t)dx \le \|u(x,t)\|^2 + \|u_t(x,t)\|^2 < \infty. \tag{43}$$

Accordingly, we can conclude that $\lim_{t\to\infty} \|w(x,t)\| = 0$, $\lim_{t\to\infty} \|v(x,t)\| = 0$, and $\lim_{t\to\infty} \|u(x,t)\| = 0$ via Lemma 3.

Furthermore, Lemmas 4 and 5 also imply

$$-e_y^2(t) \ge -W_1(t) \ge -V(t)/\lambda_1 \ge \dot{V}(t)/\lambda_1\lambda \Rightarrow \lim_{t\to\infty} \int_0^t e_y^2(\tau)d\tau \le -\lim_{t\to\infty} (V(t) - V(0))/\lambda_1\lambda < \infty, \tag{44}$$

$$-e_z^2(t) \ge -W_1(t) \ge -V(t)/\lambda_1 \ge \dot{V}(t)/\lambda_1\lambda \Rightarrow \lim_{t\to\infty} \int_0^t e_z^2(\tau)d\tau \le -\lim_{t\to\infty} (V(t) - V(0))/\lambda_1\lambda < \infty. \tag{45}$$

Based on Barbalat's Lemma, we can conclude that $\lim_{t\to\infty} |e_y| = 0$ and $\lim_{t\to\infty} |e_z| = 0$.

Inequality (30) implies the boundedness of $V(t)$. It follows that the potential energy function is also a bounded function. Under Assumption 2, $w_{xx}(x, t)$, $w_{xxx}(x, t)$, $v_{xx}(x, t)$, and $v_{xxx}(x, t)$ are bounded. Inequalities (34)-(37) reveal that e_y, $\dot{e}_y$,e_z, and $\dot{e}_z$ are also bounded. Finally, we can conclude that the control laws in (15) and (16) are bounded. Theorem 1 is proved.

Simulation results

In this section, numerical simulations are performed to illustrate the effectiveness of the proposed control laws. The system parameters used in the numerical simulation are shown in Table 1. According to these system parameters, the control gains in (15) and (16) are selected as $K_1 = 750$, $K_2 = 950$, $K_3 = 1.12 \times 10^4$, $K_4 = 550$, $K_5 = 750$, and $K_6 = 2.34 \times 10^4$. Control parameters K_i ($i = 1, 2, \ldots, 6$) are calculated based on design parameters k_i, α_n, β_j, and δ_k ($n = 1, 2, 3$; $j = 1, 2, \ldots, 7$; $k = 1, 2, \ldots, 9$). These design parameters have been selected to satisfy the conditions in (A.15–A.23), (B.9), (B.17–B.22), and (B.25–B.35). Some parameters, such as δ_1, δ_2, δ_4, and α_2, can be pre-determined based on the necessary conditions of (A.15–A.17) and (A.19). By substituting these parameters into (B.9), (B.17), and (B.20), β_1, β_3, β_6, β_7, k_3, and k_6 are calculated. Then, the ranges of β_2, δ_0, δ_3, β_4, β_8, β_5, β_9, δ_5, δ_6, δ_7, and δ_8 can be determined in turn based on (A.21–A.22), (B.19), (B.22), and (B.30)-(B.35). We substitute (B.18) into (A.22) and choose large enough values of k_1 and k_2 such that (A.22) and (B.25–B.26) hold. Similarly,

Parameter	Definition	Value
l	Beam length	1.5 m
h	Beam height	0.01 m
b	Beam width	0.006 m
A	Beam's cross-section area	0.6×10^{-4} m^2
I_y	Beam's initial moment	1.8×10^{-10} m^4
I_z	Beam's initial moment	5×10^{-10} m^4
ρ	Beam's mass density	2700 kg/m^2
E	Young's modulus	69×10^9 Pa
m_1	Gantry's mass	30 kg
m_2	Trolley's mass	20 kg
c_w	Transverse damping coefficient	0.05 Ns/m
c_v	Lateral damping coefficient	0.05 Ns/m
c_u	Longitudinal damping coefficient	0.05 Ns/m
y_d	Trolley's desired position	6 m
z_d	Gantry's desired position	4 m

Table 1. System parameters.

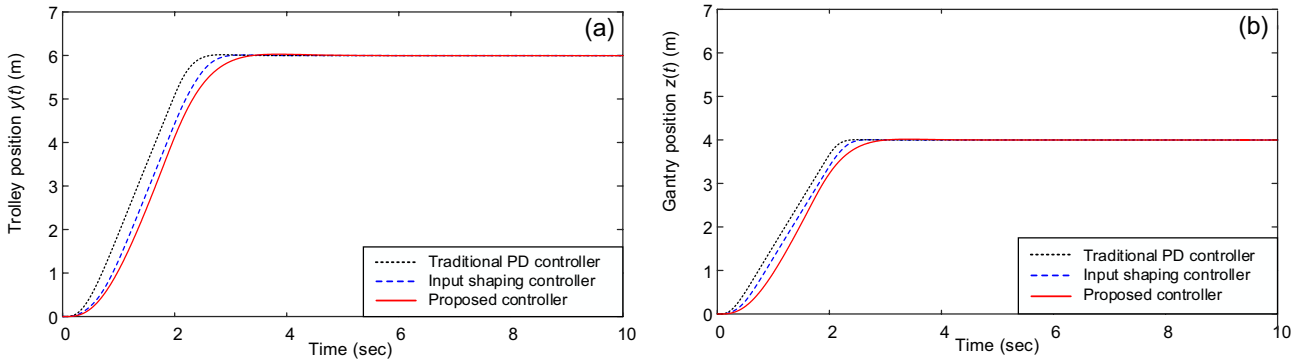

Figure 2. (**a**) Trolley's position and (**b**) gantry's position.

we substitute (B.18) into (A.23) and select k_4 and k_5 to satisfy (A.23) and (B.28–B.29). Finally, α_1 and α_3 are calculated using (B.18) and (B.21).

The simulations were performed by using MATLAB, wherein the finite difference method was utilized to determine the approximate solutions for the equations of motion. The approximate solutions' accuracy and simulation speed depend on the sizes of the time and space steps (i.e., Δt and Δx, respectively). By using a large time step size, approximate solutions of PDEs are determined quickly. However, a too-large time step size reduces the accuracy of the solution and further leads to instability. Contrarily, the quality of the solutions can be improved by selecting a smaller step size. In this case, the simulation duration increases significantly. Therefore, selecting appropriate step sizes is necessary to guarantee a balance between accuracy and simulation speed. In this paper, the time and space step sizes are selected as follows: $\Delta t = 10^{-5}$ and $\Delta x = 0.075$.

The dynamic behavior of the proposed control law (15) and (16) is compared with two typical cases: (i) Using the traditional PD control law and (ii) using the zero-vibration (ZV) input shaping control. For the input shaping control, the ZV input shapers are designed based on the cantilever beam's natural frequencies and damping ratios. The natural frequencies are determined via the solution of the frequency Eq.[26], whereas the damping ratios are calculated by using the logarithmic decrement algorithm[27].

Figures 2 and 3 illustrate the system's responses under different controllers. Figure 2 shows the trolley's position and gantry's position, whereas Fig. 3 reveal the vibrations of the beam's tip. It shows that the PD controller, input shaping controller, and the proposed controller can move the trolley and gantry to the desired position (i.e., Fig. 2). However, the traditional PD controller cannot deal with the beam's vibrations, see Fig. 3. In this case, vibration suppression was done only based on structural damping; therefore, it requires a significant amount of time. Contrary to the PD control, the system's vibrations under the input shaping control and the proposed control law were quickly suppressed, see Fig. 3. Most tip oscillations were eliminated when the trolley and gantry reached the desired positions (i.e., at $t \approx 4$ s). Furthermore, the proposed control law showed an outstanding vibration suppression capability compared with the input shaping control (i.e., see the magnified graphs in Fig. 3). The control forces under the proposed control law and suppression of the three vibrations are depicted in Figs. 4 and 5.

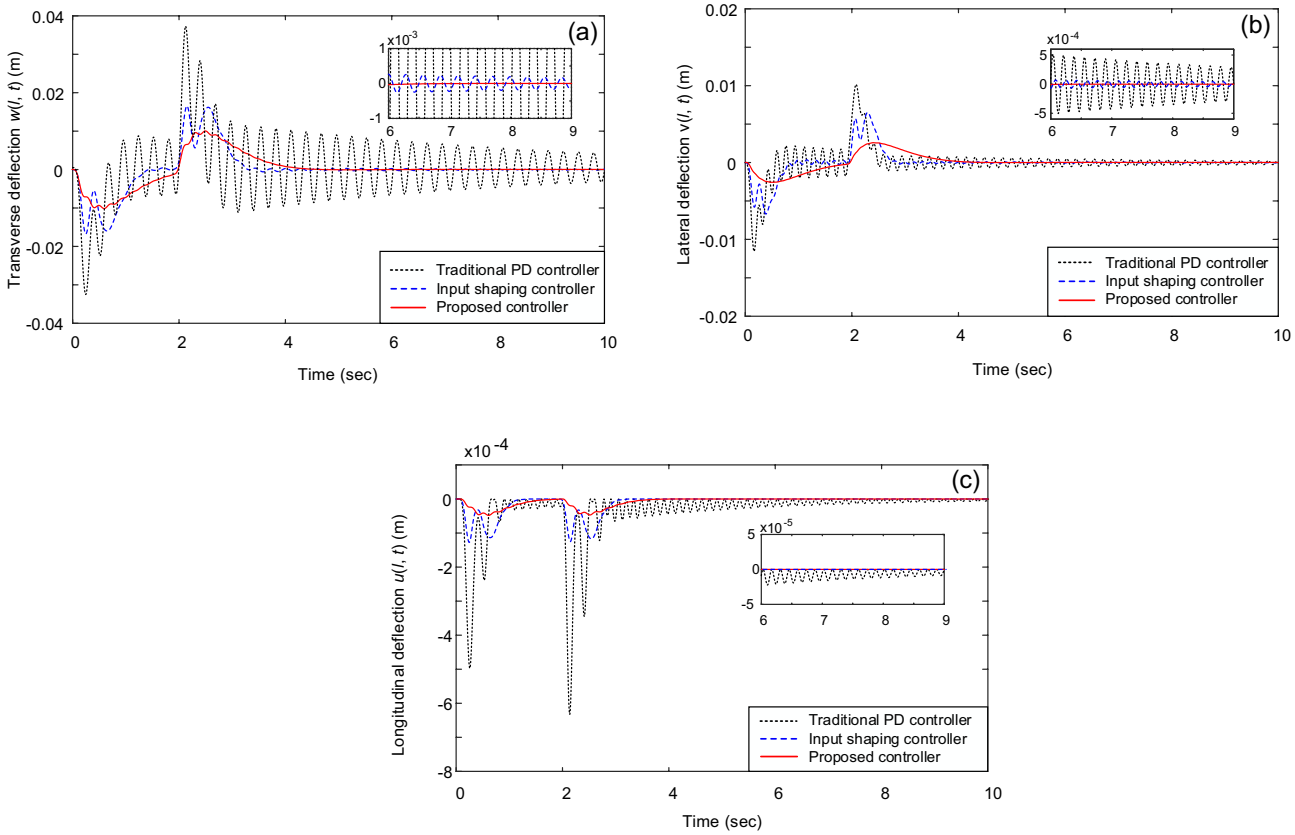

Figure 3. Vibrations of the beam's tip: (**a**) Transverse vibration $w(l, t)$, (**b**) lateral vibration $v(l, t)$, and (**c**) longitudinal vibration $u(l, t)$.

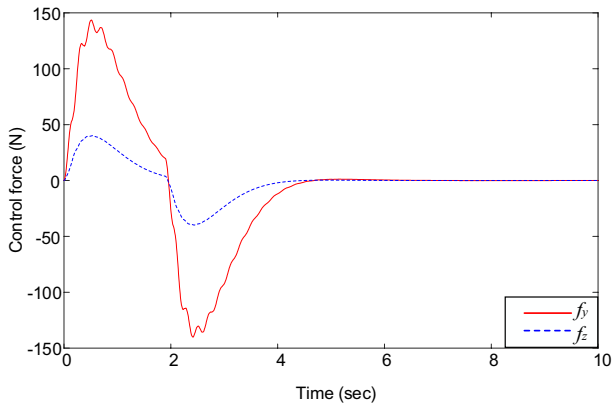

Figure 4. Control forces under the proposed control law.

Figures 6 and 7 reveal the robustness of the proposed control law. In Fig. 6, we consider the system under the influence of disturbances. Two boundary disturbances, $d_y(t) = 10\sin(20\pi t)$ and $d_z(t) = 8\sin(20\pi t)$, are applied to the trolley and gantry, respectively. As shown in Fig. 6, the proposed control law can still eliminate most of the vibrations of the beam system under boundary disturbance. The sensitivity of the proposed control law to the measurement noises of the sensors is considered in Fig. 7. In this case, 20% noises are added in the feedback signals $w_{xxx}(0, t)$ and $v_{xxx}(0, t)$. Observably, the measurement noises have no significant effects on the responses of the closed-loop system under the proposed control law. The simulation results show that the proposed control law is not too sensitive to disturbances and measurement noises.

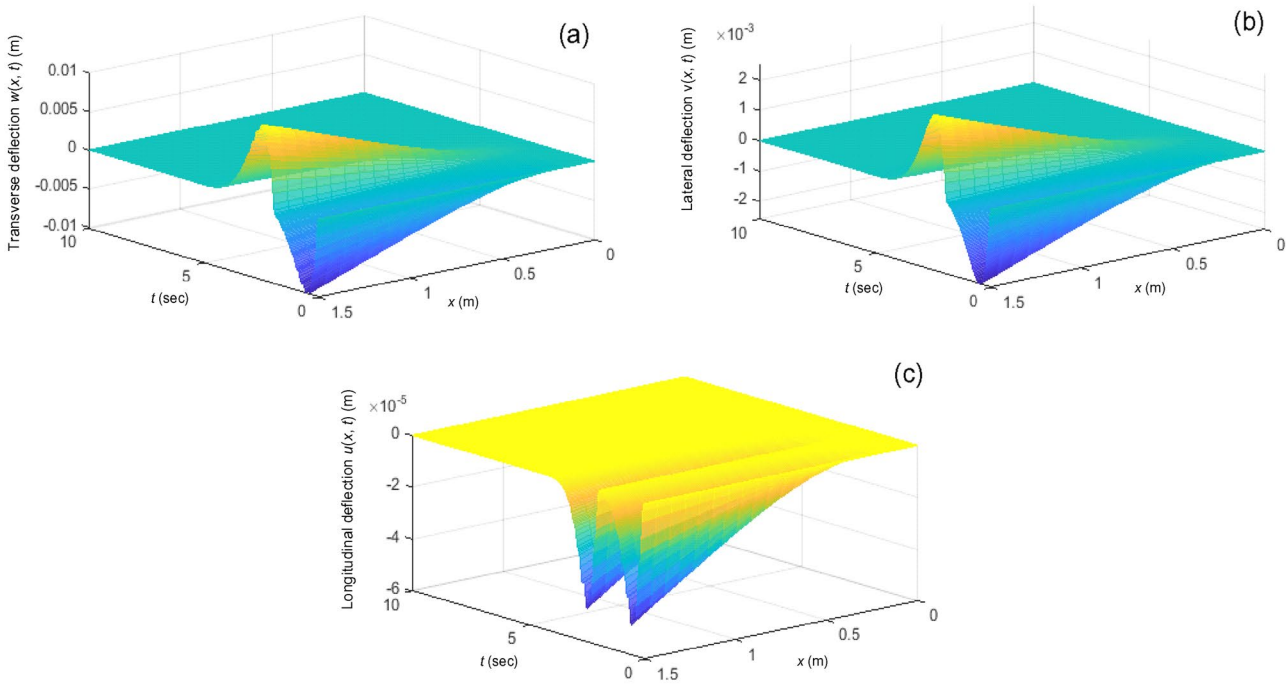

Figure 5. Vibrations of the three-dimensional flexible beam under the proposed control law: (**a**) Transverse vibration $w(x, t)$, (**b**) lateral vibration $v(x, t)$, and (**c**) longitudinal vibration $u(x, t)$.

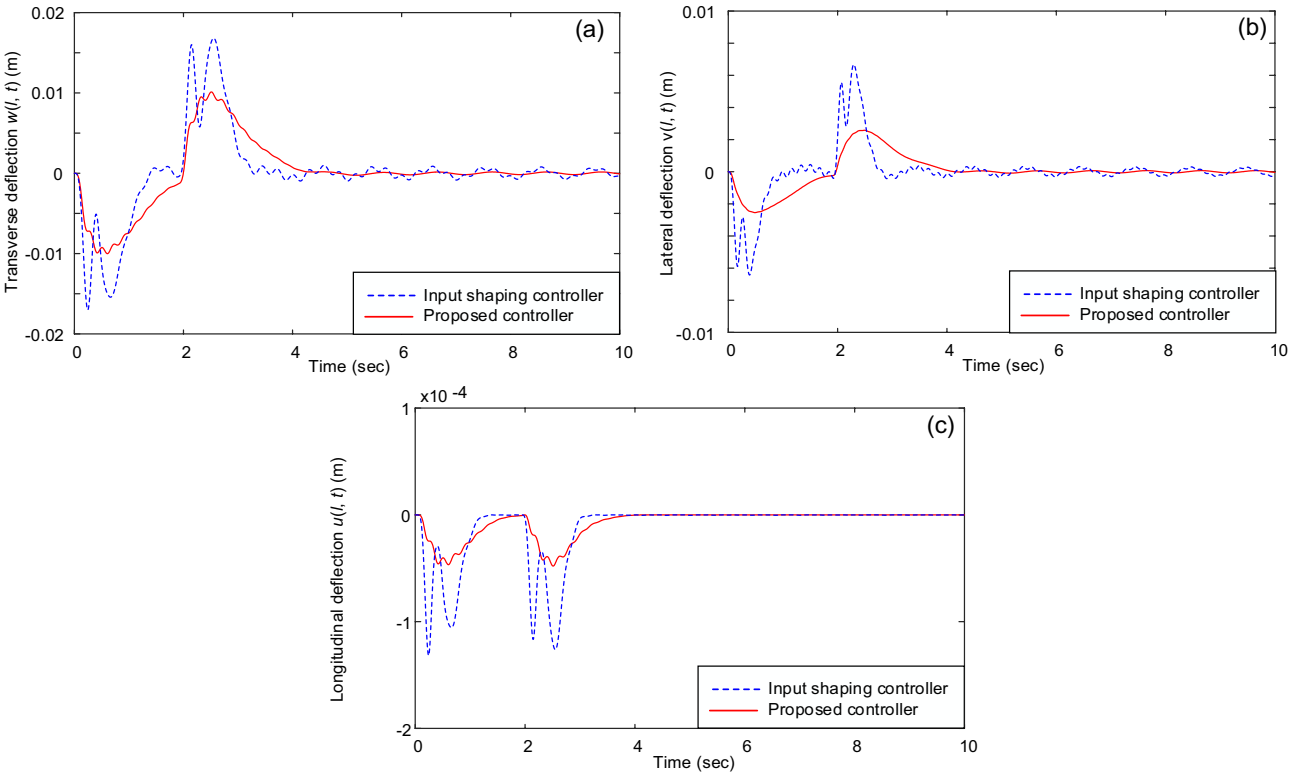

Figure 6. Vibrations of the beam's tip under boundary disturbances: (**a**) Transverse vibration $w(l, t)$, (**b**) lateral vibration $v(l, t)$, and (**c**) longitudinal vibration $u(l, t)$.

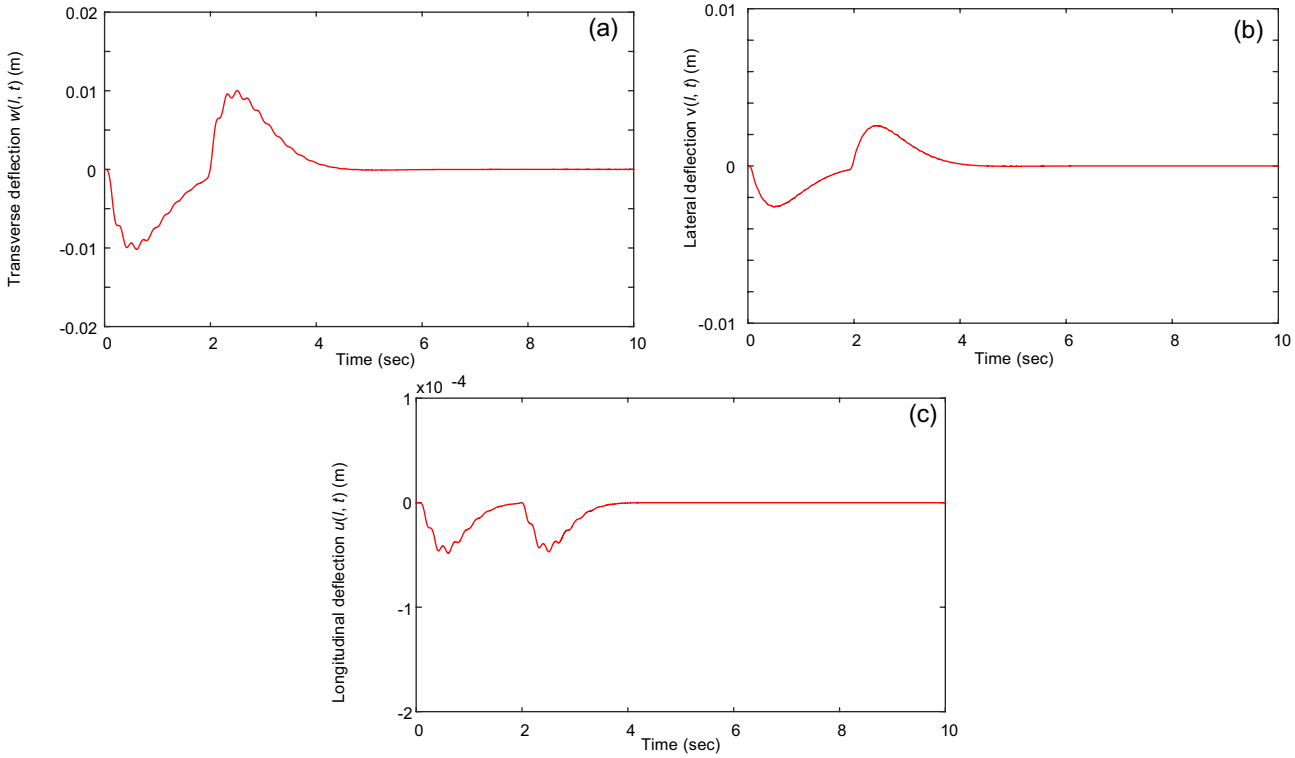

Figure 7. Vibrations of the beam's tip under measurement noises in feedback signals: (**a**) Transverse vibration $w(l, t)$, (**b**) lateral vibration $v(l, t)$, and (**c**) longitudinal vibration $u(l, t)$.

Conclusions

This paper investigated a vibration suppression problem of the three-dimensional cantilever beam fixed on a translating base. The equations of motions describing the nonlinear coupling dynamics of the beam's transverse, lateral, longitudinal vibrations, the gantry, and the trolley were developed using the Hamilton principle. Accordingly, the control laws were designed. The asymptotic stability of the closed-loop system in the sense that the beam's transverse vibration, lateral vibration, longitudinal vibration, and gantry's position error and trolley's position error converge to zero was proven via the Lyapunov method. Simulation results showed the effectiveness of the proposed control laws. In practical gantry systems, the length of the robotic arm varies in time, and the system is subjected to disturbances. Our future work will address extending the current control strategy to a varying-length flexible beam with moving base, providing experimental results.

Data availability

The data and codes generated or analyzed in this paper can be available upon the communication with the corresponding author.

Appendix A

The proof of Lemma 4 is shown in here. By using Lemmas 1–2, we obtain

$$\left|\int_0^l w w_t dx\right| \leq (l^4/\delta_0)\int_0^l w_{xx}^2 dx + \delta_0 \int_0^l w_t^2 dx, \tag{A.1}$$

$$\left|\int_0^l u u_t dx\right| \leq \frac{1}{4} l^4 \delta_1 \left(\int_0^l w_{xx}^2 dx + \int_0^l v_{xx}^2 dx\right) + \delta_1 \int_0^l u_t^2 dx, \tag{A.2}$$

$$\left|\int_0^l w \dot{y} dx\right| \leq l^4 \int_0^l w_{xx}^2 dx + l\dot{y}^2, \tag{A.3}$$

$$\left|\int_0^l \dot{y} w_t dx\right| \leq (l/\delta_2)\dot{y}^2 + \delta_2 \int_0^l w_t^2 dx, \tag{A.4}$$

$$\left|\dot{y}e_y\right| \le \dot{y}^2 + e_y^2, \tag{A.5}$$

$$\left|\int_0^l e_y(\dot{y} + w_t)dx\right| \le 2le_y^2 + l\dot{y}^2 + \int_0^l w_t^2 dx, \tag{A.6}$$

$$\left|\int_0^l v v_t dx\right| \le (l^4/\delta_3)\int_0^l v_{xx}^2 dx + \delta_3 \int_0^l v_t^2 dx, \tag{A.7}$$

$$\left|\int_0^l v\dot{z}dx\right| \le l^4 \int_0^l v_{xx}^2 dx + l\dot{z}^2, \tag{A.8}$$

$$\left|\int_0^l \dot{z}v_t dx\right| \le (l/\delta_4)\dot{z}^2 + \delta_4 \int_0^l v_t^2 dx, \tag{A.9}$$

$$|\dot{z}e_z| \le \dot{z}^2 + e_z^2, \tag{A.10}$$

$$\left|\int_0^l e_z(\dot{z} + v_t)dx\right| \le 2le_z^2 + l\dot{z}^2 + \int_0^l v_t^2 dx. \tag{A.11}$$

According to (A.1)-(A.11), the lower bound of V_0 and V_1 are given by

$$\begin{aligned} V_0 \ge{}& \frac{1}{2}\rho A\int_0^l u_t^2 dx + \left(\frac{1}{2} + \alpha_2/\rho A\right)\left[EI_y\int_0^l w_{xx}^2 dx + EI_z\int_0^l v_{xx}^2 dx\right] \\ &+\frac{1}{2}(m_1+m_2)\dot{y}^2 + \frac{1}{2}m_2\dot{z}^2 + \frac{1}{2}\alpha_1 e_y^2 + \frac{1}{2}\alpha_3 e_z^2 \\ &+\alpha_2\int_0^l w_t^2 dx + \alpha_2\int_0^l u_t^2 dx + \alpha_2\int_0^l v_t^2 dx, \end{aligned} \tag{A.12}$$

$$\begin{aligned} V_1 \ge{}& [\beta_3 l(1 - c_w/\rho A - 1/\delta_2) - \beta_4 - \beta_5 l]\dot{y}^2 \\ &+[\beta_7 l(1 - c_v/\rho A - 1/\delta_4) - \beta_8 - \beta_9 l]\dot{z}^2 \\ &-(\rho A\beta_1\delta_1 + \beta_3\delta_2 + \beta_5)\int_0^l w_t^2 dx - \rho A\delta_1\beta_2\int_0^l u_t^2 dx - (\rho A\beta_6\delta_3 + \beta_7\delta_4 + \beta_9)\int_0^l v_t^2 dx \\ &-l^4(\rho A\beta_1/\delta_1 + \rho A\beta_2/4\delta_1 + \beta_3 c_w/\rho A)\int_0^l w_{xx}^2 dx \\ &-l^4(\rho A\beta_6/\delta_3 + \beta_7 c_v/\rho A + \rho A\beta_2/4\delta_1)\int_0^l v_{xx}^2 dx \\ &-(\beta_4 + 2\beta_5 l)e_y^2 - (\beta_8 + 2\beta_9 l)e_z^2. \end{aligned} \tag{A.13}$$

Based on (A.12) and (A.13), the lower bound of the Lyapunov function candidate is obtained as follows.

$$\begin{aligned} V \ge{}& [(m_1+m_2)/2 + \beta_3 l(1 - c_w/\rho A - 1/\delta_2) - \beta_4 - \beta_5 l]\dot{y}^2 \\ &+ [m_2/2 + \beta_7 l(1 - c_v/\rho A - 1/\delta_4) - \beta_8 - \beta_9 l]\dot{z}^2 \\ &+ [\alpha_2 - (\rho A\beta_1\delta_0 + \beta_3\delta_2 + \beta_5)]\int_0^l w_t^2 dx + [\alpha_2 + \rho A/2 - \delta_1\rho A\beta_2]\int_0^l u_t^2 dx \\ &+ [\alpha_2 - (\rho A\beta_6\delta_3 + \beta_7\delta_4 + \beta_9)]\int_0^l v_t^2 dx \\ &+ \left[EI_y(1/2 + \alpha_2/\rho A) - l^4(\rho A\beta_1/\delta_0 + \rho A\beta_2/4\delta_1 + \beta_3 c_w/\rho A)\right]\int_0^l w_{xx}^2 dx \\ &+ \left[EI_z(1/2 + \alpha_2/\rho A) - l^4(\rho A\beta_6/\delta_3 + \rho A\beta_2/4\delta_1 + \beta_7 c_v/\rho A)\right]\int_0^l v_{xx}^2 dx \\ &+ [\alpha_1/2 - (\beta_4 + 2\beta_5 l)]e_y^2 + [\alpha_5/2 - (\beta_8 + 2\beta_9 l)]e_z^2 \\ \ge{}& \lambda_1 W_1 \end{aligned} \tag{A.14}$$

where $\lambda_1 = \min(\lambda_{11}, \lambda_{12}, ..., \lambda_{19})$ and α_i, β_j, and δ_k ($i = 1, 2, ..., 6$, $j = 1, 2, ..., 9$, and $k = 1, 2, ..., 4$) are selected to guarantee that λ_{1n} ($i = 1, 2, ..., 9$) satisfy

$$\lambda_{11} = (m_1 + m_2)/2 + \beta_3 l(1 - c_w/\rho A - 1/\delta_2) - \beta_4 - \beta_5 l > 0, \tag{A.15}$$

$$\lambda_{12} = m_2/2 + \beta_7 l(1 - c_v/\rho A - 1/\delta_4) - \beta_8 - \beta_9 l > 0, \tag{A.16}$$

$$\lambda_{13} = \alpha_2 - (\rho A\beta_1\delta_0 + \beta_3\delta_2 + \beta_5) > 0, \tag{A.17}$$

$$\lambda_{14} = \alpha_2 + \rho A/2 - \delta_1\rho A\beta_2 > 0, \tag{A.18}$$

$$\lambda_{15} = \alpha_2 - (\rho A\beta_6\delta_3 + \beta_7\delta_4 + \beta_9) > 0, \tag{A.19}$$

$$\lambda_{16} = EI_y(1/2 + \alpha_2/\rho A) - l^4(\rho A\beta_1/\delta_0 + \rho A\beta_2/4\delta_1 + \beta_3 c_w/\rho A) > 0, \tag{A.20}$$

$$\lambda_{17} = EI_z(1/2 + \alpha_2/\rho A) - l^4(\rho A\beta_6/\delta_3 + \rho A\beta_2/4\delta_1 + \beta_7 c_v/\rho A) > 0, \tag{A.21}$$

$$\lambda_{18} = \alpha_1/2 - (\beta_4 + 2\beta_5 l) > 0, \tag{A.22}$$

$$\lambda_{19} = \alpha_5/2 - (\beta_8 + 2\beta_9 l) > 0. \tag{A.23}$$

Similarly, the upper bound of the Lyapunov function candidate can be obtained by using (A.1)-(A.11), that is

$$\begin{aligned} V \le\ & [\rho Al + (m_1 + m_2)/2 + \beta_4 + \beta_5 l + \beta_3 l(1 + c_w/\rho A + 1/\delta_2)]\dot{y}^2 \\ & + [\rho Al + m_2/2 + \beta_8 + \beta_9 l + \beta_7 l(1 + c_v/\rho A + 1/\delta_4)]\dot{z}^2 \\ & + (\rho A + \rho A\beta_1\delta_0 + \beta_3\delta_2 + \beta_5 + \alpha_2)\int_0^l w_t^2 dx + (\rho A + \rho A\beta_6\delta_3 + \beta_7\delta_4 + \beta_9 + \alpha_2)\int_0^l v_t^2 dx \\ & + (\rho A/2 + \delta_1\rho A\beta_2 + \alpha_2)\int_0^l u_t^2 dx \\ & + (1/2 + \alpha_2/\rho A)\int_0^l P(w_x^2 + v_x^2)dx + (1/2 + \alpha_2/\rho A)EA\int_0^l (u_x + w_x^2/2 + v_x^2/2)^2 dx \\ & + \left[EI_y(1/2 + \alpha_2/\rho A) + l^4(\rho A\beta_1/\delta_0 + \beta_1 c_w/2 + \rho A\beta_2/4\delta_1 + \beta_2 c_w/8 + \beta_3 c_w/\rho A)\right]\int_0^l w_{xx}^2 dx \\ & + \left[EI_z(1/2 + \alpha_2/\rho A) + l^4(\rho A\beta_6/\delta_3 + \beta_6 c_v/2 + \rho A\beta_2/4\delta_1 + \beta_2 c_v/8 + \beta_7 c_v/\rho A)\right]\int_0^l v_{xx}^2 dx \\ & + (\alpha_1/2 + \beta_4 + 2\beta_5 l)e_y^2 + (\alpha_3/2 + \beta_8 + 2\beta_9 l)e_z^2 \\ & \le \lambda_2 W_2 \end{aligned} \tag{A.24}$$

where $\lambda_2 = \max(\lambda_{21}, \lambda_{22}, ..., \lambda_{211})$ and

$$\lambda_{21} = \rho Al + (m_1 + m_2)/2 + \beta_4 + \beta_5 l + \beta_3 l(1 + c_w/\rho A + 1/\delta_2), \tag{A.25}$$

$$\lambda_{22} = \rho Al + m_2/2 + \beta_8 + \beta_9 l + \beta_7 l(1 + c_v/\rho A + 1/\delta_4), \tag{A.26}$$

$$\lambda_{23} = \rho A + \rho A\beta_1\delta_0 + \beta_3\delta_2 + \beta_5 + \alpha_2, \tag{A.27}$$

$$\lambda_{24} = \rho A + \rho A\beta_6\delta_3 + \beta_7\delta_4 + \beta_9 + \alpha_2, \tag{A.28}$$

$$\lambda_{25} = \rho A/2 + \delta_1\rho A\beta_2 + \alpha_2, \tag{A.29}$$

$$\lambda_{26} = 1/2 + \alpha_2/\rho A, \tag{A.30}$$

$$\lambda_{27} = (1/2 + \alpha_2/\rho A)EA, \tag{A.31}$$

$$\lambda_{28} = EI_y(1/2 + \alpha_2/\rho A) + l^4(\rho A\beta_1/\delta_0 + \beta_1 c_w/2 + \rho A\beta_2/4\delta_1 + \beta_2 c_w/8 + \beta_3 c_w/\rho A), \tag{A.32}$$

$$\lambda_{29} = EI_z(1/2 + \alpha_2/\rho A) + l^4(\rho A\beta_6/\delta_3 + \beta_6 c_v/2 + \rho A\beta_2/4\delta_1 + \beta_2 c_v/8 + \beta_7 c_v/\rho A), \tag{A.33}$$

$$\lambda_{210} = \alpha_1/2 + \beta_4 + 2\beta_5 l, \tag{A.34}$$

$$\lambda_{211} = \alpha_3/2 + \beta_8 + 2\beta_9 l. \tag{A.35}$$

Based on (A.14–A.23) and (A.24–A.25), Lemma 4 is proven.

Appendix B

The proof of Lemma 5 is shown here. The time derivative of V_0 is derived as follows.

$$\begin{aligned}\dot{V}_0 = {} & \rho A \int_0^l (\dot{y} + w_t)(\ddot{y} + w_{tt})dx + \rho A \int_0^l (\dot{z} + v_t)(\ddot{z} + v_{tt})dx + \rho A \int_0^l u_t u_{tt} dx \\ & + (1 + 2\alpha_2/\rho A)\left[\int_0^l P(w_x w_{xt} + v_x v_{xt})dx + EA \int_0^l \left(u_x + w_x^2/2 + v_x^2/2\right)(u_{xt} + w_x w_{xt} + v_x v_{xt})dx \right. \\ & \left. + EI_y \int_0^l w_{xx} w_{xxt} dx + EI_z \int_0^l v_{xx} v_{xxt} dx\right] + (m_1 + m_2)\dot{y}\ddot{y} + m_2 \dot{z}\ddot{z} + \alpha_1 e_y \dot{y} + \alpha_3 e_z \dot{z} \\ & + 2\alpha_2 \left(\int_0^l w_t w_{tt} dx + \int_0^l u_t u_{tt} dx + \int_0^l v_t v_{tt} dx\right).\end{aligned} \tag{B.1}$$

For notational convenience, ε is used instead of $(u_x + w_x^2/2 + v_x^2/2)$ (i.e., ε is the axial strain given in (3)). Substituting the dynamic model in (5)-(12) into (B.1) yields

$$\begin{aligned}\dot{V}_0 = {} & -c_w \int_0^l w_t^2 dx - c_u \int_0^l u_t^2 dx - c_v \int_0^l v_t^2 dx - c_w \int_0^l \dot{y} w_t dx - c_v \int_0^l \dot{z} v_t dx \\ & + \left[P w_x \dot{y}\right]\Big|_0^l + \left[P v_x \dot{z}\right]\Big|_0^l + \left[EA\varepsilon w_x \dot{y}\right]\Big|_0^l + \left[EA\varepsilon v_x \dot{z}\right]\Big|_0^l - \left[EI_y \dot{y} w_{xxx}\right]\Big|_0^l - \left[EI_z \dot{z} v_{xxx}\right]\Big|_0^l \\ & + (1 + 2\alpha_2/\rho A)\Big\{\left[P w_x w_t\right]\Big|_0^l + \left[P v_x v_t\right]\Big|_0^l + \left[EA\varepsilon u_t\right]\Big|_0^l + \left[EA\varepsilon w_x w_t\right]\Big|_0^l + \left[EA\varepsilon v_x v_t\right]\Big|_0^l \\ & + EI_y \left[w_{xx} w_{xt} - w_t w_{xxx}\right]\Big|_0^l + EI_z \left[v_{xx} v_{xt} - v_t v_{xxx}\right]\Big|_0^l\Big\} + (m_1 + m_2)\dot{y}\ddot{y} + m_2 \dot{z}\ddot{z} \\ & - (2c_w \alpha_2/\rho A) \int_0^l w_t^2 dx - (2c_u \alpha_2/\rho A) \int_0^l u_t^2 dx - (2c_v \alpha_2/\rho A) \int_0^l v_t^2 dx \\ & - 2\alpha_2 \ddot{y} \int_0^l w_t dx - 2\alpha_2 \ddot{z} \int_0^l v_t dx + \alpha_1 e_y \dot{y} + \alpha_3 e_z \dot{z}.\end{aligned} \tag{B.2}$$

By using the boundary conditions and $P(l) = 0$, (B.2) can be rewritten as

$$\begin{aligned}\dot{V}_0 = {} & -c_w \int_0^l w_t^2 dx - c_u \int_0^l u_t^2 dx - c_v \int_0^l v_t^2 dx - \dot{y} c_w \int_0^l w_t dx - \dot{z} c_v \int_0^l v_t dx + EI_y \dot{y} w_{xxx}(0,t) + EI_z \dot{z} v_{xxx}(0,t) \\ & + (m_1 + m_2)\dot{y}\ddot{y} + m_2 \dot{z}\ddot{z} - (2c_w \alpha_2/\rho A) \int_0^l w_t^2 dx - (2c_u \alpha_2/\rho A) \int_0^l u_t^2 dx - (2c_v \alpha_2/\rho A) \int_0^l v_t^2 dx \\ & - 2\alpha_2 \ddot{y} \int_0^l w_t dx - 2\alpha_2 \ddot{z} \int_0^l v_t dx + \alpha_1 e_y \dot{y} + \alpha_3 e_z \dot{z} \\ = {} & -c_w (1 + 2\alpha_2/\rho A) \int_0^l w_t^2 dx - c_u (1 + 2\alpha_2/\rho A) \int_0^l u_t^2 dx - c_v (1 + 2\alpha_2/\rho A) \int_0^l v_t^2 dx + \dot{y} f_y + \dot{z} f_z \\ & - 2\alpha_2 \ddot{y} \int_0^l w_t dx - 2\alpha_2 \ddot{z} \int_0^l v_t dx + \alpha_1 e_y \dot{y} + \alpha_3 e_z \dot{z}.\end{aligned} \tag{B.3}$$

The time derivative of V_1 is derived as follows.

$$\begin{aligned}\dot{V}_1 &= \rho A\beta_1 \int_0^l w_t^2 dx + \rho A\beta_1 \int_0^l w w_{tt} dx + \beta_1 c_w \int_0^l w w_t dx + \rho A\beta_2 \int_0^l u_t^2 dx + \rho A\beta_2 \int_0^l u u_{tt} dx + \beta_2 c_u \int_0^l u u_t dx \\ &+ (\beta_3 c_w/\rho A) \int_0^l w_t \dot{y} dx + (\beta_3 c_w/\rho A) \int_0^l w\ddot{y} dx + \beta_3 \int_0^l \ddot{y}(\dot{y} + w_t) dx + \beta_3 \int_0^l \dot{y}(\ddot{y} + w_{tt}) dx + \beta_4 \ddot{y} e_y \\ &+ \beta_4 \dot{y}^2 + \beta_5 \int_0^l \dot{y}(\dot{y} + w_t) dx + \beta_5 \int_0^l e_y(\ddot{y} + w_{tt}) dx + \rho A\beta_6 \int_0^l v_t^2 dx + \rho A\beta_6 \int_0^l v v_{tt} dx + \beta_6 c_v \int_0^l v v_t dx \\ &+ (\beta_7 c_v/\rho A) \int_0^l v_t \dot{z} dx + (\beta_7 c_v/\rho A) \int_0^l v\ddot{z} dx + \beta_7 \int_0^l \ddot{z}(\dot{z} + v_t) dx + \beta_7 \int_0^l \dot{z}(\ddot{z} + v_{tt}) dx + \beta_8 \ddot{z} e_z \\ &+ \beta_8 \dot{z}^2 + \beta_9 \int_0^l \dot{z}(\dot{z} + v_t) dx + \beta_9 \int_0^l e_z(\ddot{z} + v_{tt}) dx.\end{aligned} \tag{B.4}$$

Using the dynamic model and boundary conditions in (5)-(12) yields

$$\begin{aligned}\dot{V}_1 &= (\beta_4 + \beta_5 l)\dot{y}^2 + (\beta_8 + \beta_9 l)\dot{z}^2 + \rho A\beta_1 \int_0^l w_t^2 dx + \rho A\beta_2 \int_0^l u_t^2 dx + \rho A\beta_6 \int_0^l v_t^2 dx \\ &+ \beta_1 \int_0^l w(Pw_x)_x dx + \beta_1 \int_0^l w(EA\varepsilon w_x)_x dx + \beta_2 \int_0^l EAu\varepsilon_x dx + \beta_6 \int_0^l v(Pv_x)_x dx \\ &+ \beta_6 \int_0^l v(EA\varepsilon v_x)_x dx - EI_y\beta_1 \int_0^l w w_{xxxx} dx - EI_z\beta_6 \int_0^l v v_{xxxx} dx + (c_w\beta_3 l/(m_1 + m_2) \\ &+ \beta_5) \int_0^l \dot{y} w_t dx + (c_w\beta_4/(m_1 + m_2) - c_w\beta_5/\rho A) \int_0^l e_y w_t dx \\ &+ (c_v\beta_7 l/m_2 + \beta_9) \int_0^l \dot{z} v_t dx + (c_v\beta_8/m_2 - c_v\beta_9/\rho A) \int_0^l e_z v_t dx \\ &+ (\beta_3 c_w/\rho A - \rho A\beta_1) \int_0^l w\ddot{y} dx + (\beta_7 c_v/\rho A - \rho A\beta_6) \int_0^l v\ddot{z} dx \\ &+ \beta_3 \int_0^l \ddot{y} w_t dx + \beta_7 \int_0^l \ddot{z} v_t dx + (\beta_3 l/(m_1 + m_2))\dot{y} f_y \\ &+ (\beta_4/(m_1 + m_2))e_y f_y + (\beta_7 l/m_2)\dot{z} f_z + (\beta_8/m_2)e_z f_z \\ &+ EI_y(\beta_3/\rho A - \beta_3 l/(m_1 + m_2))\dot{y} w_{xxx}(0,t) + EI_y(\beta_5/\rho A - \beta_4/(m_1 + m_2))e_y w_{xxx}(0,t) \\ &+ EI_z(\beta_7/\rho A - l\beta_7/m_2)\dot{z} v_{xxx}(0,t) + EI_z(\beta_9/\rho A - \beta_8/m_2)e_z v_{xxx}(0,t).\end{aligned} \tag{B.5}$$

According to (B.3) and (B.5), the time derivative of V is derived as follows.

$$\begin{aligned}\dot{V} &= \dot{y}\big[(\beta_3 l/(m_1 + m_2) + 1)f_y + (\beta_4 + \beta_5 l)\dot{y} + EI_y(\beta_3/\rho A - \beta_3 l/(m_1 + m_2))w_{xxx}(0,t) + \alpha_1 e_y\big] \\ &+ \dot{z}\big[(\beta_7 l/m_2 + 1)f_z + (\beta_8 + \beta_9 l)\dot{z} + EI_z(\beta_7/\rho A - l\beta_7/m_2)v_{xxx}(0,t) + \alpha_3 e_z\big] \\ &- [c_w(1 + 2\alpha_2/\rho A) - \rho A\beta_1] \int_0^l w_t^2 dx - [c_u(1 + 2\alpha_2/\rho A) - \rho A\beta_2] \int_0^l u_t^2 dx \\ &- [c_v(1 + 2\alpha_2/\rho A) - \rho A\beta_6] \int_0^l v_t^2 dx \\ &+ \beta_1 \int_0^l w(Pw_x)_x dx + \beta_1 \int_0^l w(EA\varepsilon w_x)_x dx - EI_y\beta_1 \int_0^l w w_{xxxx} dx + \beta_2 \int_0^l EAu\varepsilon_x dx \\ &+ \beta_6 \int_0^l v(Pv_x)_x dx + \beta_6 \int_0^l v(EA\varepsilon v_x)_x dx - EI_z\beta_6 \int_0^l v v_{xxxx} dx \\ &+ (\beta_3 c_w/\rho A - \rho A\beta_1) \int_0^l w\ddot{y} dx + (c_w\beta_3 l/(m_1 + m_2) + \beta_5) \int_0^l \dot{y} w_t dx \\ &+ (\beta_7 c_v/\rho A - \rho A\beta_6) \int_0^l v\ddot{z} dx + (\beta_7 l c_v/m_2 + \beta_9) \int_0^l \dot{z} v_t dx \\ &- c_w(\beta_5/\rho A - \beta_4/(m_1 + m_2) \int_0^l e_y w_t dx - c_v(\beta_9/\rho A - \beta_8/m_2) \int_0^l e_z v_t dx \\ &+ (\beta_3 - 2\alpha_2)\ddot{y} \int_0^l w_t dx + EI_y(\beta_5/\rho A - \beta_4/(m_1 + m_2))e_y w_{xxx}(0,t) + (\beta_4/(m_1 + m_2))e_y f_y \\ &+ (\beta_7 - 2\alpha_2)\ddot{z} \int_0^l v_t dx + EI_z(\beta_9/\rho A - \beta_8/m_2)e_z v_{xxx}(0,t) + (\beta_8/m_2)e_z f_z.\end{aligned} \tag{B.6}$$

By using integration by parts and Lemma 1, the following inequality and equation are obtained.

$$\begin{aligned}
&\beta_1\int_0^l w(Pw_x)_x dx+\beta_1\int_0^l w(EA\varepsilon w_x)_x dx+\beta_2\int_0^l u(EA\varepsilon u_x)_x dx\\
&\quad+\beta_6\int_0^l v(Pv_x)_x dx+\beta_6\int_0^l v(EA\varepsilon v_x)_x dx\\
&\quad\le-\beta_1\int_0^l Pw_x^2 dx-\beta_6\int_0^l Pv_x^2 dx+\delta_5 EAl^2\left(\int_0^l w_{xx}^2 dx+\int_0^l v_{xx}^2 dx\right)\\
&\quad-\left(\beta_2-\left((2\beta_1-\beta_2)^2+(2\beta_6-\beta_2)^2\right)/4\delta_5\right)EA\int_0^l \varepsilon^2 dx,
\end{aligned}\tag{B.7}$$

$$-\beta_1 EI_y\int_0^l ww_{xxxx}dx=-\beta_1 EI_y\int_0^l w_{xx}^2 dx;\ -EI_z\beta_6\int_0^l vv_{xxxx}dx=-\beta_6 EI_z\int_0^l v_{xx}^2 dx\tag{B.8}$$

where δ_5 is a positive constant. It is noted that the inequalities $w_x^4\ll w_x^2$ and $v_x^4\ll v_x^2$ are used in (B.7). By letting β_i satisfy the following conditions

$$\beta_3=\beta_7=2\alpha_2\beta_3 c_w/\rho A=\rho A\beta_1,\ \beta_7 c_v/\rho A=\rho A\beta_6,\ \beta_5/\rho A-\beta_4/(m_1+m_2)\ge 0,\ \beta_9/\rho A-\beta_8/m_2\ge 0\tag{B.9}$$

and using Lemmas 1 and 2 for the terms $\int_0^l \dot{y}w_t dx$, $\int_0^l e_y w_t dx$, $\int_0^l \dot{z}v_t dx$, and $\int_0^l e_z v_t dx$ of (B.6), we obtain

$$\begin{aligned}
\dot{V}\le&-[c_w(1+2\alpha_2/\rho A)-\rho A\beta_1-c_w\delta_7(\beta_5/\rho A-\beta_4/(m_1+m_2))\ -\delta_6(c_w\beta_3 l/(m_1+m_2)+\beta_5)]\int_0^l w_t^2 dx\\
&-[c_u(1+2\alpha_2/\rho A)\ -\rho A\beta_2]\int_0^l u_t^2 dx\\
&-[c_v(1+2\alpha_2/\rho A)\ -\rho A\beta_6-\delta_9 c_v(\beta_9/\rho A-\beta_8/m_2)-\delta_8(\beta_7 lc_v/m_2+\beta_9)]\int_0^l v_t^2 dx\\
&-\left(\beta_1 EI_y-\delta_5 EAl^2\right)\int_0^l w_{xx}^2 dx-\left(\beta_6 EI_z-\delta_5 EAl^2\right)\int_0^l v_{xx}^2 dx\\
&-\max(\beta_1,\beta_6)\int_0^l P\left(w_x^2+v_x^2\right)dx-\left(\beta_2-\left((2\beta_1-\beta_2)^2+(2\beta_6-\beta_2)^2\right)/4\delta_5\right)\int_0^l EA\varepsilon^2 dx+D_y+D_z
\end{aligned}\tag{B.10}$$

where

$$\begin{aligned}
D_y=&\left[(\beta_3 l/(m_1+m_2)+1)f_y+((c_w\beta_3 l/(m_1+m_2)+\beta_5)l/\delta_6+\beta_4+\beta_5 l)\dot{y}\right.\\
&\left.+EI_y(\beta_3/\rho A-\beta_3 l/(m_1+m_2))w_{xxx}(0,t)+\alpha_1 e_y\right]\dot{y}\\
&+(c_w l(\beta_5/\rho A-\beta_4/(m_1+m_2))/\delta_7)e_y^2+EI_y(\beta_5/\rho A-\beta_4/(m_1+m_2))e_y w_{xxx}(0,t)\\
&+(\beta_4/(m_1+m_2))e_y f_y,
\end{aligned}\tag{B.11}$$

$$\begin{aligned}
D_z=&\left[(\beta_7 l/m_2+1)f_z+(\beta_8+\beta_9 l+(\beta_7 lc_v/m_2+\beta_9)l/\delta_8)\dot{z}\right.\\
&\left.+EI_z(\beta_7/\rho A-\beta_7 l/m_2)v_{xxx}(0,t)+\alpha_3 e_z\right]\dot{z}\\
&+(c_v l(\beta_9/\rho A-\beta_8/m_2)/\delta_9)e_z^2+EI_z(\beta_9/\rho A-\beta_8/m_2)e_z v_{xxx}(0,t)+(\beta_8/m_2)e_z f_z.
\end{aligned}\tag{B.12}$$

In (B.10–B.12), δ_i ($i=6, 7, 8, 9$) are positive constants. Substituting the control laws in (15) and (16) into (B.11) and (B.12), respectively, yields

$$\begin{aligned}
D_y=&-[k_1-\beta_4-\beta_5 l-(c_w\beta_3 l/(m_1+m_2)+\beta_5)l/\delta_6]\dot{y}^2\\
&-[k_2\beta_4/(\beta_3 l+m_1+m_2)-c_w l(\beta_5/\rho A\ -\beta_4/(m_1+m_2))/\delta_7]e_y^2\\
&+\left(\beta_3 EI_y/\rho A-\beta_3 lEI_y/(m_1+m_2)-k_3)\dot{y}w_{xxx}(0,t)+(\alpha_1-k_2-k_1\beta_4/(\beta_3 l+m_1+m_2))e_y\dot{y}\right.\\
&+\left(\beta_5 EI_y/\rho A-\beta_4 EI_y/(m_1+m_2)-k_3\beta_4/(\beta_3 l+m_1+m_2))e_y w_{xxx}(0,t),\right.
\end{aligned}\tag{B.13}$$

$$\begin{aligned}
D_z=&-[k_4-\beta_8-\beta_9 l-(\beta_7 lc_v/m_2+\beta_9)l/\delta_8]\dot{z}^2\\
&-[k_5\beta_8/(\beta_7 l+m_2)-c_v l(\beta_9/\rho A-\beta_8/m_2)/\delta_9]e_z^2\\
&+(\beta_7 EI_z/\rho A-\beta_7 lEI_z/m_2-k_6)\dot{z}v_{xxx}(0,t)+(\alpha_3-k_5-k_4\beta_8/(\beta_7 l+m_2))e_z\dot{z}\\
&+(\beta_9 EI_z/\rho A-\beta_8 EI_z/m_2-k_6\beta_8/(\beta_7 l+m_2))e_z v_{xxx}(0,t)
\end{aligned}\tag{B.14}$$

where

$$k_i=(\beta_3 l/(m_1+m_2)+1)K_i,\ i=1,2,3,\tag{B.15}$$

$$k_j = (\beta_7 l/m_2 + 1)K_j,\ j = 4, 5, 6. \tag{B.16}$$

If the following conditions hold

$$EI_y(\beta_3/\rho A - \beta_3 l/(m_1 + m_2)) - k_3 = 0, \tag{B.17}$$

$$\alpha_1 - k_2 - k_1\beta_4/(\beta_3 l + m_1 + m_2) = 0, \tag{B.18}$$

$$EI_z(\beta_9/\rho A - \beta_8/m_2) - k_6\beta_8/(\beta_7 l + m_2) = 0, \tag{B.19}$$

$$EI_z(\beta_7/\rho A - \beta_7 l/m_2) - k_6 = 0, \tag{B.20}$$

$$\alpha_3 - k_5 - k_4\beta_8/(\beta_7 l + m_2) = 0, \tag{B.21}$$

$$EI_y(\beta_5/\rho A - \beta_4/(m_1 + m_2)) - k_3\beta_4/(\beta_3 l + m_1 + m_2) = 0 \tag{B.22}$$

then (B.10) can be rewritten as follows.

$$\begin{aligned}
\dot{V} \le & -[k_1 - \beta_4 - \beta_5 l - (c_w\beta_3 l/(m_1 + m_2) + \beta_5)l/\delta_6]\dot{y}^2 \\
& - [k_4 - \beta_8 - \beta_9 l - (\beta_7 l c_v/m_2 + \beta_9)l/\delta_8]\dot{z}^2 \\
& - [k_2\beta_4/(\beta_3 l + m_1 + m_2) - c_w l(\beta_5/\rho A - \beta_4/(m_1 + m_2))/\delta_7]e_y^2 \\
& - [k_5\beta_8/(\beta_7 l + m_2) - c_v l(\beta_9/\rho A - \beta_8/m_2)/\delta_9]e_z^2 \\
& - [c_w(1 + 2\alpha_2/\rho A) - \rho A\beta_1 - \delta_6(c_w\beta_3 l/(m_1 + m_2) + \beta_5) - c_w\delta_7(\beta_5/\rho A - \beta_4/(m_1 + m_2))]\int_0^l w_t^2 dx \\
& - [c_v(1 + 2\alpha_2/\rho A) - \rho A\beta_6 - \delta_8(c_v\beta_7 l/m_2 + \beta_9) - \delta_9 c_v(\beta_9/\rho A - \beta_8/m_2)]\int_0^l v_t^2 dx \\
& - [c_u(1 + 2\alpha_2/\rho A) - \rho A\beta_2]\int_0^l u_t^2 dx - E\left(\beta_1 I_y - \delta_5 A l^2\right)\int_0^l w_{xx}^2 dx - E\left(\beta_6 I_z - \delta_5 A l^2\right)\int_0^l v_{xx}^2 dx \\
& - \max(\beta_1, \beta_6)\int_0^l P(w_x^2 + v_x^2)dx - \left(\beta_2 - \left((2\beta_1 - \beta_2)^2 + (2\beta_6 - \beta_2)^2/4\delta_5\right)\right)\int_0^l EA\varepsilon^2 dx.
\end{aligned} \tag{B.23}$$

Inequality (B.23) leads to the following result

$$\dot{V} \le -\lambda_3 W_2 \tag{B.24}$$

where $\lambda_3 = \min(\lambda_{31}, \lambda_{32}, ..., \lambda_{311})$ and coefficients α_i, β_j, and δ_k ($i = 1, 2, \ldots, 6$, $j = 1, 2, \ldots, 9$, and $k = 1, 2, \ldots, 8$) satisfy the conditions:

$$\lambda_{31} = k_1 - \beta_4 - \beta_5 l - (c_w\beta_3 l/(m_1 + m_2) + \beta_5)l/\delta_6 \ge 0, \tag{B.25}$$

$$\lambda_{32} = k_2\beta_4/(\beta_3 l + m_1 + m_2) - c_w(\beta_5/\rho A - \beta_4/(m_1 + m_2))l/\delta_7 \ge 0, \tag{B.26}$$

$$\lambda_{33} = \max(\beta_1, \beta_6) \ge 0, \tag{B.27}$$

$$\lambda_{34} = k_4 - \beta_8 - \beta_9 l - l(c_v\beta_7 l/m_2 + \beta_9)/\delta_8 \ge 0, \tag{B.28}$$

$$\lambda_{35} = k_5\beta_8/(\beta_7 l + m_2) - c_v l(\beta_9/\rho A - \beta_8/m_2)/\delta_9 \ge 0, \tag{B.29}$$

$$\lambda_{36} = c_u(1 + 2\alpha_2/\rho A) - \rho A\beta_2 \ge 0, \tag{B.30}$$

$$\lambda_{37} = c_w(1 + 2\alpha_2/\rho A) - \rho A\beta_1 - \delta_6(c_w\beta_3 l/(m_1 + m_2) + \beta_5) - c_w\delta_7(\beta_5/\rho A - \beta_4/(m_1 + m_2) \ge 0, \tag{B.31}$$

$$\lambda_{38} = c_v(1 + 2\alpha_2/\rho A) - \rho A\beta_6 - \delta_8(c_v\beta_7 l/m_2 + \beta_9) - \delta_9 c_v(\beta_9/\rho A - \beta_8/m_2) \ge 0, \tag{B.32}$$

$$\lambda_{39} = E\left(\beta_1 I_y - \delta_5 A l^2\right) \ge 0, \tag{B.33}$$

$$\lambda_{310} = E\left(\beta_6 I_z - \delta_5 A l^2\right) \ge 0, \tag{B.34}$$

$$\lambda_{311} = \beta_2 - \left((2\beta_1 - \beta_2)^2 + (2\beta_6 - \beta_2)^2\right)/4\delta_5 \ge 0. \tag{B.35}$$

Based on Lemma 4, the following inequality is derived

$$\dot{V} \leq -\lambda_3 W_2 \leq -(\lambda_3/\lambda_2)V \Rightarrow \dot{V} \leq -\lambda V \tag{B.36}$$

where $\lambda = \lambda_3/\lambda_2$. Accordingly, Lemma 5 is proven.

Received: 31 March 2022; Accepted: 19 July 2022
Published online: 15 August 2022

References

1. Kim, B. & Chung, J. Residual vibration reduction of a flexible beam deploying from a translating hub. *J. Sound Vib.* **333**(16), 3759–3775 (2014).
2. Mustafazade, A. *et al.* A vibrating beam MEMS accelerometer for gravity and seismic measurements. *Sci. Rep.* **10**, 10415 (2020).
3. Gao, N., Zhao, D., Jia, R. & Liu, D. Microcantilever actuation by laser induced photoacoustic waves. *Sci. Rep.* **6**, 19935 (2016).
4. Yang, R. *et al.* Nanoscale cutting using self-excited microcantilever. *Sci. Rep.* **12**, 618 (2022).
5. Pham, P.-T. & Hong, K.-S. Dynamic models of axially moving systems: A review. *Nonlinear Dyn.* **100**(1), 315–349 (2020).
6. Wang, H., Wang, X., Yang, W. & Du, Z. Design and kinematic modeling of a notch continuum manipulator for laryngeal surgery. *Int. J. Control Autom. Syst.* **18**(11), 2966–2973 (2020).
7. Veryaskin, A. V. & Meyer, T. J. Static and dynamic analyses of free-hinged-hinged-hinged-free beam in non-homogeneous gravitational field: Application to gravity gradiometry. *Sci. Rep.* **12**, 7215 (2022).
8. Eshag, M. A., Ma, L., Sun, Y. & Zhang, K. Robust boundary vibration control of uncertain flexible robot manipulator with spatiotemporally-varying disturbance and boundary disturbance. *Int. J. Control Autom. Syst.* **19**(2), 788–798 (2021).
9. Hanagud, S. & Sarkar, S. Problem of the dynamics of a cantilevered beam attached to a moving base. *J. Guid. Control Dyn.* **12**(3), 438–441 (1989).
10. Huang, J. S., Fung, R. F. & Tseng, C. R. Dynamic stability of a cantilever beam attached to a translational/rotational base. *J. Sound Vib.* **224**(2), 221–242 (1999).
11. Park, S., Kim, B. K. & Youm, Y. Single-mode vibration suppression for a beam-mass-cart system using input preshaping with a robust internal-loop compensator. *J. Sound Vib.* **241**(4), 693–716 (2001).
12. Cai, G. P., Hong, J. Z. & Yang, S. X. Dynamic analysis of a flexible hub-beam system with tip mass. *Mech. Res. Commun.* **32**(2), 173–190 (2005).
13. Park, S., Chung, W. K., Youm, Y. & Lee, J. W. Natural frequencies and open-loop responses of an elastic beam fixed on a moving cart and carrying an intermediate lumped mass. *J. Sound Vib.* **230**(3), 591–615 (2000).
14. Park, S. & Youm, Y. Motion of a moving elastic beam carrying a moving mass-analysis and experimental verification. *J. Sound Vib.* **240**(1), 131–157 (2001).
15. Shah, U. H. & Hong, K.-S. Active vibration control of a flexible rod moving in water: Application to nuclear refueling machines. *Automatica* **93**, 231–243 (2018).
16. Wu, D., Endo, T. & Matsuno, F. Exponential stability of two Timoshenko arms for grasping and manipulating an object. *Int. J. Control Autom. Syst.* **19**(3), 1328–1339 (2021).
17. Shin, K. & Brennan, M. J. Two simple methods to suppress the residual vibrations of a translating or rotating flexible cantilever beam. *J. Sound Vib.* **312**(1–2), 140–150 (2008).
18. Han, F. & Jia, Y. Sliding mode boundary control for a planar two-link rigid-flexible manipulator with input disturbances. *Int. J. Control Autom. Syst.* **18**(2), 351–362 (2020).
19. Yang, L. J. & Guo, Y. P. Output feedback stabilisation for an ODE-heat cascade systems subject to boundary control matched disturbance. *Int. J. Control Autom. Syst.* **19**(11), 3611–3621 (2021).
20. Nguyen, Q. C., Piao, M. & Hong, K.-S. Multivariable adaptive control of the rewinding process of a roll-to-roll system governed by hyperbolic partial differential equations. *Int. J. Control Autom. Syst.* **16**(5), 2177–2186 (2018).
21. Nguyen, Q. C. & Hong, K.-S. Simultaneous control of longitudinal and transverse vibrations of an axially moving string with velocity tracking. *J. Sound Vib.* **331**(13), 3006–3019 (2012).
22. Zhou, Y., Cui, B. & Lou, X. Dynamic H∞ feedback boundary control for a class of parabolic systems with a spatially varying diffusivity. *Int. J. Control Autom. Syst.* **19**(2), 999–1012 (2021).
23. Wang, L. & Jin, F. F. Boundary output feedback stabilization of the linearized Schrödinger equation with nonlocal term. *Int. J. Control Autom. Syst.* **19**(4), 1528–1538 (2021).
24. Fu, M., Zhang, T. & Ding, F. Adaptive safety motion control for underactuated hovercraft using improved integral barrier lyapunov function. *Int. J. Control Autom. Syst.* **19**(8), 2784–2796 (2021).
25. Xia, H., Chen, J., Lan, F. & Liu, Z. Motion control of autonomous vehicles with guaranteed prescribed performance. *Int. J. Control Autom. Syst.* **18**(6), 1510–1517 (2020).
26. Shah, U. H., Hong, K.-S. & Choi, S. H. Open-loop vibration control of an underwater system: Application to refueling machine. *IEEE-ASME Trans. Mechatron.* **22**(4), 1622–1632 (2017).
27. Pham, P.-T., Kim, G.-H., Nguyen, Q. C. & Hong, K.-S. Control of a non-uniform flexible beam: Identification of first two modes. *Int. J. Control Autom. Syst.* **19**(11), 3698–3707 (2021).
28. Lin, J. & Chao, W. S. Vibration suppression control of beam-cart system with piezoelectric transducers by decomposed parallel adaptive neuro-fuzzy control. *J. Vib. Control* **15**(12), 1885–1906 (2009).
29. Qiu, Z. C. Adaptive nonlinear vibration control of a Cartesian flexible manipulator driven by a ballscrew mechanism. *Mech. Syst. Signal Proc.* **30**, 248–266 (2012).
30. Hong, K.-S., Chen, L.-Q., Pham, P.-T. & Yang, X.-D. *Control of Axially Moving Systems* (Springer, 2021).
31. Hong, K.-S. & Pham, P.-T. Control of axially moving systems: A review. *Int. J. Control Autom. Syst.* **17**(12), 2983–3008 (2019).
32. Sun, C., He, W. & Hong, J. Neural network control of a flexible robotic manipulator using the lumped spring-mass model. *IEEE Trans. Syst. Man Cybern. Syst.* **47**(8), 1863–1874 (2017).
33. Khot, S. M., Yelve, N. P., Tomar, R., Desai, S. & Vittal, S. Active vibration control of cantilever beam by using PID based output feedback controller. *J. Vib. Control* **18**(3), 366–372 (2012).
34. Pham, P. T., Kim, G.-H. & Hong, K.-S. Vibration control of a Timoshenko cantilever beam with varying length. *Int. J. Control Autom. Syst.* **20**(1), 175–183 (2022).
35. Liu, Z. & Liu, J. *PDE Modeling and Boundary Control for Flexible Mechanical System* 137–171 (Springer, 2020).
36. Ji, N., Liu, Z., Liu, J. & He, W. Vibration control for a nonlinear three-dimensional Euler-Bernoulli beam under input magnitude and rate constraints. *Nonlinear Dyn.* **91**(4), 2551–2570 (2018).
37. Zhang, Y., Liu, J. & He, W. Vibration control for a nonlinear three-dimensional flexible manipulator trajectory tracking. *Int. J. Control* **89**(8), 1641–1663 (2016).
38. Do, K. D. & Pan, J. Boundary control of three-dimensional inextensible marine risers. *J. Sound Vib.* **327**(3–5), 299–321 (2009).
39. Do, K. D. Boundary control design for extensible marine risers in three-dimensional space. *J. Sound Vib.* **388**, 1–19 (2017).

40. Ge, S. S., He, W., How, B. V. E. & Choo, Y. S. Boundary control of a coupled nonlinear flexible marine riser. *IEEE Trans. Control Syst. Technol.* **18**(5), 1080–1091 (2009).
41. He, W., Yang, C., Zhu, J., Liu, J. K. & He, X. Active vibration control of a nonlinear three-dimensional Euler–Bernoulli beam. *J. Vib. Control* **23**(19), 3196–3215 (2017).
42. Ji, N. & Liu, J. Adaptive neural network control for a nonlinear Euler–Bernoulli beam in three-dimensional space with unknown control direction. *Int. J. Robust Nonlinear Control* **29**(13), 4494–4514 (2019).
43. Ji, N. & Liu, J. Vibration and event-triggered control for flexible nonlinear three-dimensional Euler–Bernoulli beam system. *J. Comput. Nonlinear Dyn.* **15**(11), 111007 (2020).
44. Liu, Z., Liu, J. & He, W. Boundary control of an Euler–Bernoulli beam with input and output restrictions. *Nonlinear Dyn.* **92**(2), 531–541 (2018).
45. Zhu, W. D., Ni, J. & Huang, J. Active control of translating media with arbitrarily varying length. *J. Vib. Acoust.* **123**(3), 347–358 (2001).
46. Zhu, W. D. & Ni, J. Energetics and stability of translating media with an arbitrarily varying length. *J. Vib. Acoust.* **122**(3), 295–304 (2000).
47. Ghayesh, M. H. & Farokhi, H. Nonlinear dynamical behavior of axially accelerating beams: Three-dimensional analysis. *J. Comput. Nonlinear Dyn.* **11**(1), 011010 (2016).
48. Hardy, G. H., Littlewood, J. E. & Polya, G. *Inequalities* (Cambridge University Press, 1959).
49. Rahn, C. D. *Mechanical Control of Distributed Noise and Vibration* (Springer, 2001).
50. Hong, K.-S. & Bentsman, J. Direct adaptive control of parabolic systems: Algorithm synthesis and convergence and stability analysis. *IEEE Trans. Autom. Control* **39**(10), 2018–2033 (1994).
51. Queiroz, M. S., Dawson, D. M., Nagarkatti, S. P. & Zhang, F. *Lyapunov Based Control of Mechanical Systems* (Birkhauser, 2000).

Acknowledgements

This work was supported by the Korea Institute of Energy Technology Evaluation and Planning under the Ministry of Trade, Industry and Energy, Korea (South) (grant no. 20213030020160). We acknowledge Ho Chi Minh City University of Technology (HCMUT), VNU-HCM for supporting this study.

Author contributions

P.-T. Pham derived the entire mathematical equations and wrote the first draft manuscript, Q. C. Nguyen reviewed the manuscript, M. Yoon reviewed the manuscript, and K.-S. Hong conceived the idea, supervised the project, and revised the manuscript.

Competing interests

The authors declare no competing interests.

Additional information

Correspondence and requests for materials should be addressed to K.-S.H.

Reprints and permissions information is available at www.nature.com/reprints.

Publisher's note Springer Nature remains neutral with regard to jurisdictional claims in published maps and institutional affiliations.